Enhanced electrokinetic extraction of heavy metals from soils assisted by ion exchange membranes

Won-Seok Kim[a], Soon-Oh Kim[b], Kyoung-Woong Kim[a],*

[a] *Arsenic Geoenvironment Laboratory (NRL), Department of Environmental Science and Engineering, Gwangju Institute of Science and Technology (GIST), 1 Oryong-dong, Buk-gu, Gwangju 500-712, Republic of Korea*
[b] *Department of Earth and Environmental Sciences, Gyeongsang National University, 900 Gazwa-dong, Jinju 660-701, Republic of Korea*

Abstract

The potential of electrokinetic remediation technology has been successfully demonstrated for the remediation of heavy metal contaminated fine-grained soils through laboratory scale and field application studies. Various enhancement techniques have been proposed and used in order to further improve the remediation process. However, it has been reported that such enhancement schemes can create other obstacles, such as the introduction of non-target ions into the system and thereby decrease the efficiency of the remediation process. Electrokinetic soil remediation technology enhanced by an ion exchange membrane (IEM), IEM-enhanced EK processing, was experimentally evaluated for the purpose of overcoming these obstacles. In particular, this study focused on observations of a fouling problem and its settlement using an auxiliary solution cell (ASC). In addition, the efficacies of two different types of electrode configurations, rectangular and cylindrical, were investigated. The experimental results indicate that the effectiveness of the technology was increased by an enhancement scheme using an IEM. This may be explained by the prevention of metal precipitation in the region near the cathode originating from hydroxide ions generated by the electrolysis of water in the cathode. The experimental results also imply that placement of the ASC can nullify the fouling problem within the cation exchange membranes used in IEM-enhanced EK processing, and thus improve the overall effectiveness of the process. The experimental results indicate that the cylindrical electrode configuration can be implemented in practical situations to improve the treatability of cathode effluent containing a high level of contaminants after processing.
© 2004 Elsevier B.V. All rights reserved.

Keywords: Contaminated soil; Electrokinetic soil processing; Heavy metal; Ion exchange membrane

1. Introduction

Heavy metal pollution of soil and ground water is a worldwide problem [1]. Soils can be contaminated with heavy metals derived from various sources, including waste from abandoned mining, improper treatment of industrial wastes, incomplete collection of used batteries, leakage of landfill leachate, accidental spills and military activities [2]. Contamination often affects a large volume of soil underlying several areas. There are also various types of contaminated areas, such as paddy fields, farms, factory sites, residential districts and mining fields. Contaminants migrating from these sources threaten the health of human inhabitants in the local area and the ground water supply [3]. However, technologies for decontaminating these sites have not been adequately developed. In addition, it has been reported recently that soil contamination is increasing in various sites, such as residential areas near industrial complexes and reservoirs of drinking water.

Methods for cleaning up heavy metal contaminated sites involve either long-term containment or removal processing. Containment techniques are interim solutions because of the possibility of future leaks. As the contaminants in such instances are only confined or immobilized, the subsequent use of these sites is often restricted or prohibited. With in

* Corresponding author. Tel.: +82 62 970 2442; fax: +82 62 970 2434.
E-mail address: kwkim@gist.ac.kr (K.-W. Kim).

situ treatment systems, such as soil flushing, chemical treatment, and bioremediation, contaminants in fine-grained soils cannot be effectively removed due to their low hydraulic conductivities. The electrokinetic (EK) technique is one of the most promising decontamination processes and has a high efficiency and time-effectiveness in low-permeable media such as sludge and clay soils. EK soil processing is also referred to as electrokinetic remediation, electroreclamation, and electrochemical decontamination, and the significance of this method is its low operation cost and potential applicability to a wide range of contaminant types [4]. EK soil processing is envisioned as a technique to effect the removal/separation of organic and inorganic contaminants and radionuclides. The potential of this technique for waste remediation has resulted in several studies [5–11].

During EK processing, hydroxides are inevitably precipitated by the hydroxyl ions generated through the electrolysis of water in a cathode compartment, and these precipitates prevent the removal of contaminants. In order to remove and avoid precipitation in the cathode compartment, various enhancement techniques have been proposed and implemented. Hsu [7] summarized a number of enhancement techniques proposed by many researchers, which include: (1) injection of enhancing agents such as acetic acid or use of a hydroxyl ion selective membrane in the cathode reservoir to prevent precipitation or solubilize precipitates of cationic metal contaminants near the cathode [12–14]; (2) conditioning the anode and/or the cathode reservoirs to control the pH and zeta potential, enhance desorption, and increase the electroosmotic flow rate to increase mobility of contaminants [13,15–17]; (3) adding or mixing strongly complexing agents such as ammonia, citrate, and EDTA into soil, which compete with soil for metal contaminants to form soluble complexes [15,18–20]. Among the enhancement technologies proposed thus far, the scheme involving the prevention of metal precipitation has received the greatest focus and experimental evaluation. If an acidic agent is used as a cathode electrolyte to prevent hydroxide ions from flowing into a soil bed, the current efficiency decreases due to the introduction of new ions into the treated systems. In order to overcome the decrease in current efficiency due to use of an acidic catholyte, EK processing enhanced by electrodialysis (ED) was developed.

The ED is an ion exchange membrane (IEM) separation process in which an electrical potential is used as a driving force [21]. The IEMs used in the ED processing can be categorized into two types: cation exchange membranes (CEMs) that essentially allow only cations to pass through, and anion exchange membranes (AEMs) that only allow anions to pass. The configuration of conventional ED processing is schematically shown in Fig. 1a. A typical ED stack consists of a number of cells that can be divided into two groups: the concentrated compartment in which the ions are collected and the electrolyte is continuously concentrated, and the diluted compartment in which the ions are removed and the electrolyte is diluted during the processing period. The solution containing ions, which may be sodium and chloride ions as
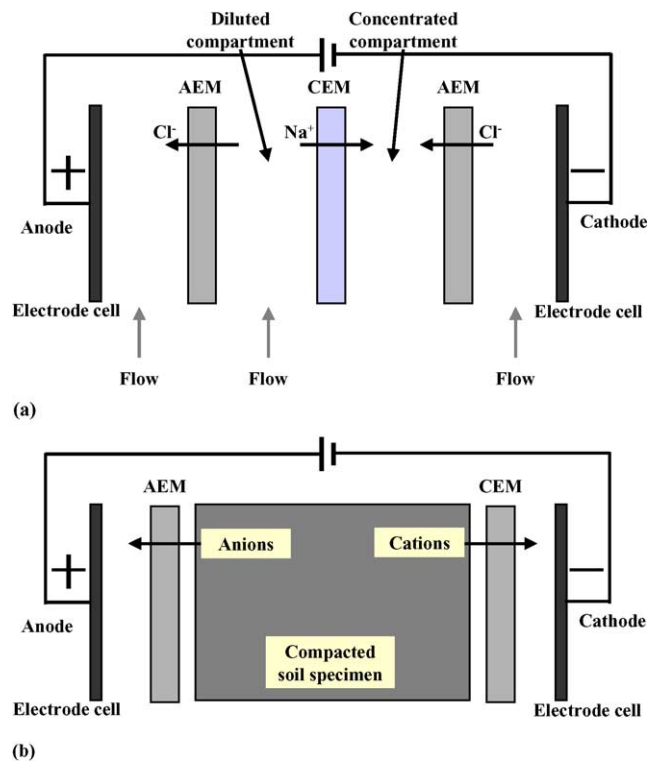

Fig. 1. Schematic diagrams showing (a) standard electrodialysis demineralization process and (b) electrodialytic (IEM-enhanced EK) soil process (AEM, anion exchange membrane; CEM, cation exchange membrane).

shown in Fig. 1a, flows through the channels. When an electric field is applied transverse to the membrane, cations and anions pass through CEM and AEM, respectively. In spite of the current appraisals of ED, fouling of IEM is one of the most crucial limitations in the design and operation of an ED process [22]. Fouling is essentially caused by the deposition of foulants on the membrane surface, causing deterioration of membrane performance through a decline in the flux and an increase in the resistance.

The IEM-enhanced EK processing is shown schematically in Fig. 1b. Based on the same principle of the ED processing, the contaminated soil is considered a diluted compartment in IEM-enhanced EK processing, as shown in Fig. 1b. The IEM-enhanced EK processing is closely connected to the ED processing. However, the two methods are different in terms of the role of the IEMs used. The IEMs play an active role in separating and concentrating ions in the ED processing, whereas they act as passive barriers to prevent ions from flowing into the soil bed from the electrode compartments. In other words, the IEMs are used in the IEM-enhanced EK processing to increase current efficiency and to prevent precipitation of hydroxides. Due to the hydrogen ions generated by electrolysis of water at the anode, an acidic solution is formed in the anodic cell. In the same manner, hydroxide ions are generated at the cathode. However, the hydroxide ions are prevented from crossing the CEM. EK processing can be improved through an enhancement involving the use of IEMs. In addition, the introduction of non-target ions into

the soil bed can be prevented by IEMs, and therefore the current efficiency of IEM-enhanced EK processing increases.

The objectives of this study were to investigate the feasibility of EK processing enhanced by IEMs for the removal of heavy metals from clay soils, to observe fouling phenomena within IEMs, and to overcome fouling phenomena by using an auxiliary solution cell (ASC). The cylindrical configuration of EK processing was also evaluated.

2. Materials and methods

Schematic diagrams and dimensions of the experimental apparatus used are shown in Figs. 2 and 3. The experimental apparatus consists of four principal parts: soil cell, electrode compartments, electrolyte solution reservoirs, and power supply. Each electrode compartment contained a sufficient volume of electrolyte solution to avoid sudden variations of pH in the electrolyte solution. One type of electrolyte solution, 0.01 M KNO_3, was recirculated in both electrode compartments using peristaltic pumps (Masterflex, 1–100 rpm, three heads), and the experimental design included the use of a BIORAD dc power supply (Model PowerPac 200, 5–200 V, 0.01–2 A, 200 W).

A set of control (conventional) and IEM-enhanced tests were undertaken using both rectangular and cylindrical electrode configurations. A number of investigations on EK processing have used the rectangular electrode configuration,
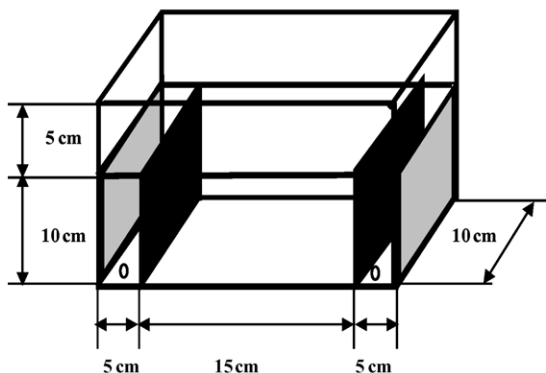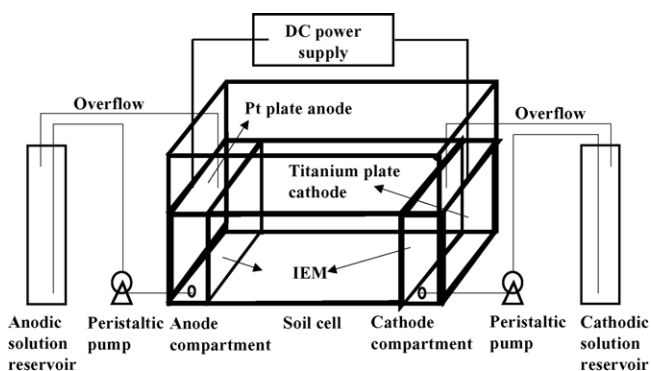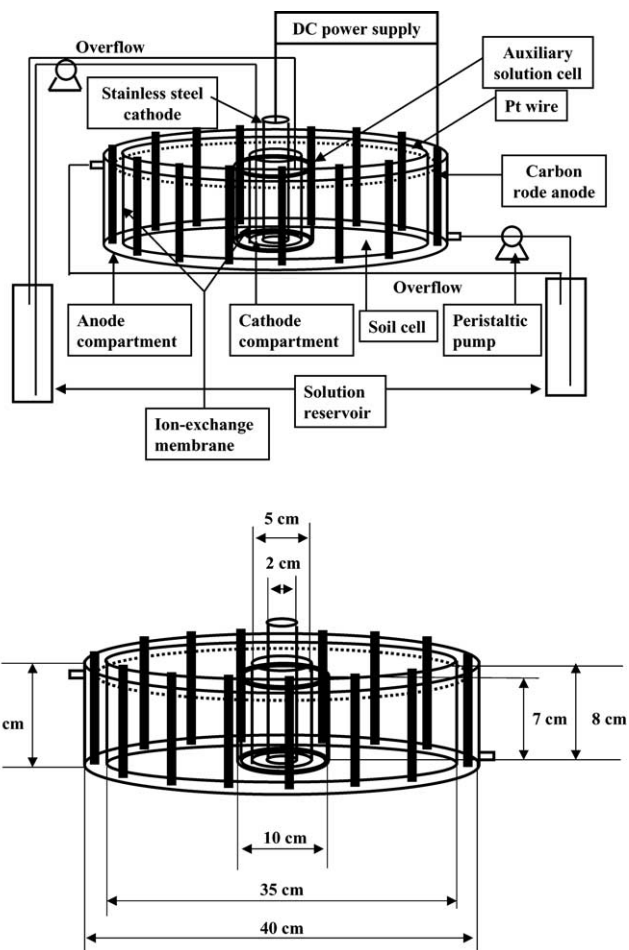

Fig. 3. A schematic diagram and dimension of the cylindrical reactor.

but few studies have employed the cylindrical configuration. However, it has been reported that the cylindrical electrode configuration can improve the treatability of contaminated cathodic effluent when EK processing is implemented in the field. It is for this reason that the cylindrical reactor was tested to evaluate the applicability of the cylindrical configuration during EK processing. Control tests were conducted using glass microfiber filters (GF/C, number 4, Whatman International Ltd.), whereas IEM-enhanced tests were undertaken using homogeneous IEMs (Neosepta, Japan). The characteristics of the IEMs tested are summarized in Table 1. Most of commercial IEMs can be categorized into homogeneous or heterogeneous IEM, according to their structure and preparation procedure. The homogeneous IEMs are produced by polymerization of functional monomers, while the heterogeneous IEMs are produced by melting and pressing of dry ion exchange resins with granulated polymers or by dispersion of ion exchange resins in the solution and melting of matrix polymers. In general, heterogeneous IEMs have relatively high electrical resistance, but the homogeneous IEMs have a more even distribution of fixed ions and often lower electrical resistance. Accordingly, the homogenous IEMs have been frequently used in the electrodialytic (ED) processing. For

Fig. 2. A schematic diagram and dimension of the rectangular reactor.

Table 1
The characteristics of commercial ion exchange membranes (Neosepta, Japan)

	Cation exchange membrane (CMX)	Anion exchange membrane (AMX)
Water content (%)	20–30	20–30
IX capacity (mequiv./g)	1.8–2.0	1.5–1.8
Transport number	0.97	0.97
Thickness (wet; mm)	0.16–0.20	0.14–0.18
Burst strength (MPa)	3.5–6.0	4.5–5.5
Characteristics	Na-form	Cl-form
	High mechanical strength	High mechanical strength

this reason, the homogenous IEMs were tested in this study. The glass fiber filters and the IEMs were inserted in the interface between the soil bed and electrode compartments in the control and IEM-enhanced tests, respectively. Furthermore, an auxiliary solution cell (ASC) was tested in the cylindrical configuration of the IEM-enhanced experiments for the purpose of preventing fouling phenomena within the IEMs. The hydroxide ions generated by cathodic water electrolysis cannot pass the cation exchange membranes (CEMs) or move into the soil bed, whereas metal contaminants can migrate from the soil bed into the cathodic electrolytes through the CEMs in the IEM-enhanced experiments. Accordingly, the metal contaminants are precipitated with the hydroxide ions within the CEMs, as well as in the cathodic electrolytes. Therefore, metal hydroxide precipitates cause the fouling phenomena within the CEMs. In order to prevent precipitation on CEM surfaces, small holes (position of hole: 2.5 cm from bottom; hole diameter: 0.2 mm; number of holes: 6; gap between holes: 2.61 cm) were added to the CEMs. A number of hydroxide ions can move from the cathodic electrolyte into the ASC through these holes, and as a consequence, metal contaminants are precipitated in the ASC rather than in the cathode electrolytes. The fouling within CEMs can therefore be prevented by the placement of an ASC between the soil bed and the cathode compartment including CEMs in the IEM-enhanced experiments. The location and dimension of the ASC are presented in Figs. 3 and 4, respectively.

Kaolinite was chosen for this study since it is one of the most ubiquitous clay soils in Korea and is commonly used as a soil medium in electrokinetic processing due to its extremely low permeability and low adsorption capacity for heavy metals in comparison with other clayey soils. The kaolinite used in experiments was commercially obtained from the Dongyang Science Co., Kwangju, Korea. Table 2 summarizes the physical properties of kaolinite soils used. The kaolinite soil was artificially contaminated with $Cd(NO_3)_2 \cdot 4H_2O$ and $Pb(NO_3)_2$ solutions, with the final concentrations of cadmium and lead in kaolinite samples being 1500 and 5000 mg/kg, respectively. All the slurries (moisture content of 50 wt.%) of kaolinite prepared for this study were mixed mechanically for 1 h with an electric stirrer; the mixtures were then allowed to settle for more than 1 week to allow for the uniform distribution of contaminants and the
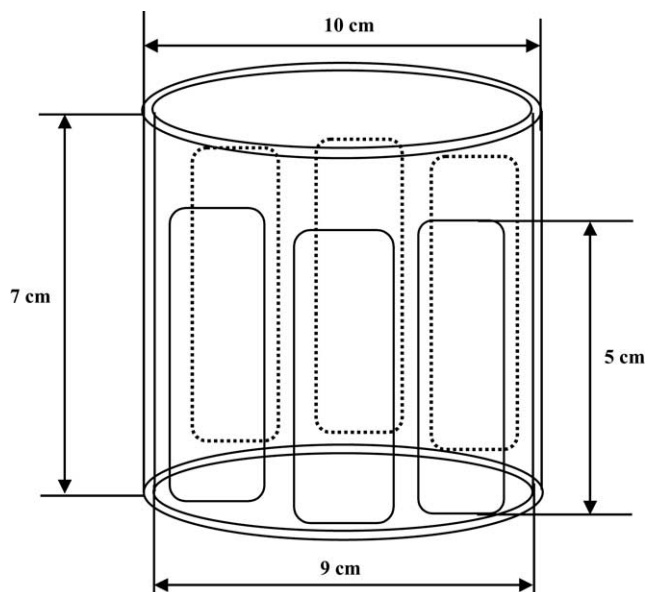

Fig. 4. Dimension of the auxiliary solution cell (ASC).

completion of adsorption in the soil samples. Five grams of six samples were then taken from the prepared soils for the determination of initial concentration of contaminants.

A number of physicochemical parameters were measured every 4 h during the experiments: the overall voltage drops of the soil cell and electrode compartments; pH variations of both electrolyte solutions; soil pH variation and transported pore water volume by electroosmotic flow. In particular, the voltage drop within CEMs was measured in IEM-enhanced tests over the period of the experiment in order to observe fouling phenomena within the CEMs. After treatment, five samples were obtained directly from the soil bed using a stainless steel sampler (diameter: 1.2 cm) to determine the residual concentrations of contaminants and final soil pHs. Fig. 5 shows the location of sampling points. Heavy metals in the soil samples were extracted using the Korea Standard Testing Method (KSTM); wet soil samples were dried at 105 °C, 50 mL of a 0.1 M HCl solution was added to 5 g of each dry soil sample (dilution factor: 10) and then agitated (100 rpm, 30 °C and 1 h). Concentrations of heavy metal contaminants were analyzed by ICP-AES (Thermo Jarrel Ash, USA).

Five tests were designed and conducted to evaluate the removal of heavy metals from soils by EK processing. The experimental program and parameters used in each test are

Table 2
Physical properties of kaolinite soils used in this study [3]

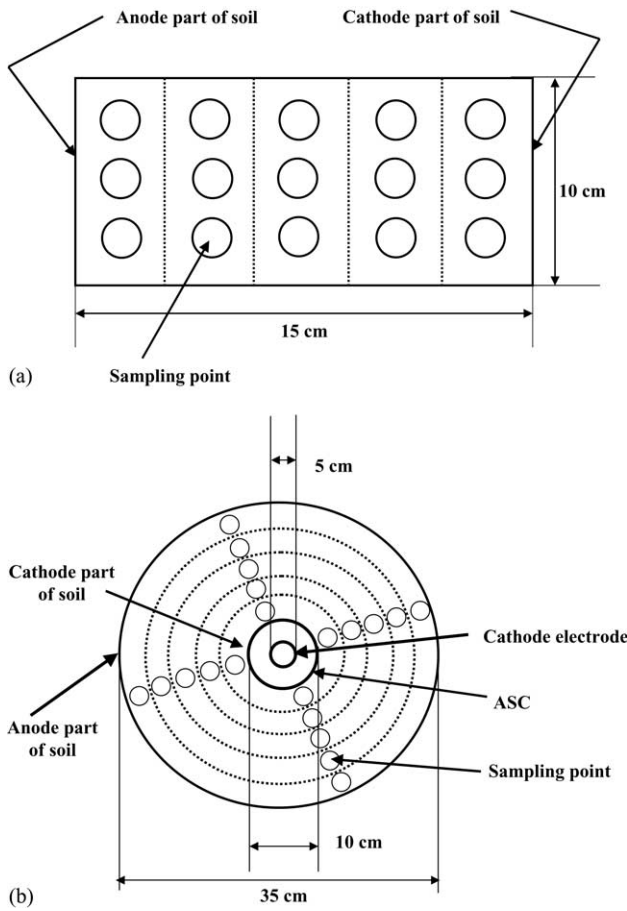| Physical property	Measured value
Group symbol according to USCS	CL
Liquid limit (%)	78
Plastic limit (%)	32
Specific gravity	2.64
PH of soil at 50% water content	4.93–5.20
Permeability (cm/s)	1×10^{-7}
Initial water content (%)	50–54

Fig. 5. A plane showing location of sampling points: (a) rectangular reactor: test 1 (control) and test 2 (IEM-enhanced); (b) cylindrical reactor: test 3 (control), test 4 (IEM-enhanced, without ASC), and test 5 (IEM-enhanced, with ASC).
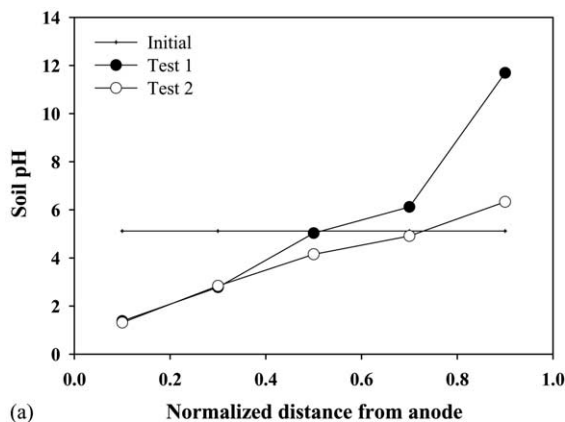
summarized in Table 3. Constant-current mode was used in all tests to keep the net rates of electrolytic reactions constant and to minimize complicated current-boundary conditions.
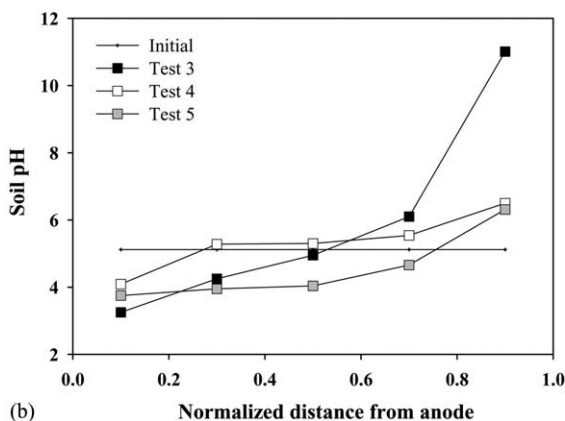
3. Results and discussion

Variations of pH in the soil bed are shown in Fig. 6. Since the transport rate of hydrogen ions is about twice that of hydroxyl ions [12,23], the pH jump point (pH = 7), in which hydrogen ions meet with hydroxyl ions, is seen near the cathode region, unless enhancing schemes are applied. For this reason, the pH jump points in the control experiments (tests 1 and 3) appear at a normalized distance from the anode of about 0.8, as shown in Fig. 6. In addition, the electroosmosis is normal (from the anode towards the cathode) in the initial stage of treatment; this electroosmotic advection also accounts for the pH jump point near the cathode region. In the cathode region, the soil pH values increased significantly (pH = 11–12) due to transport of hydroxyl ions from the cathode. This transport of base front from the cathode to the soil media brings about several detrimental effects that result in a

Table 3
Summary of experimental program and measured parameters for electrokinetic removal of heavy metals

Reactor type	Rectangular configuration		Cylindrical configuration		
	Test 1 (control)	Test 2 (IEM-enhanced)	Test 3 (control)	Test 4 (IEM-enhanced)	Test 5 (IEM-enhanced)
Anode and cathode membrane	GF/C filter	IEMs (Neosepta, Japan)	GF/C filter	IEMs (Neosepta, Japan)	IEMs (Neosepta, Japan)
Auxiliary solution cell	Without	Without	Without	Without	With
Anode electrode	Platinum plate, 10 cm (W) × 10 cm (L)		Carbon rode, 0.6 cm (∅) × 10 cm (L)		
Cathode electrode	Titanium plate, 10 cm (W) × 10 cm (L)		Stainless steel pipe, 2 cm (∅) × 15 cm (L)		
Current (A)	0.1	0.1	0.5	0.5	0.5
Dimension	10 cm (H) × 10 cm (W); volume = 1500 cm³		34 cm (∅) × 5 cm (H); volume = 4441 cm³		
Length of soil cell (cm)	15	15	14.5	14.5	12
Cross-sectional area of soil cell (cm²)	100	100	Anodic side: 534.07; cathodic side: 78.54		Anodic side: 534.07; cathodic side: 157.08
Soil specimen	Kaolinite				
Metal contaminants and initial concentration	Cadmium: Cd(NO₃)₂·4H₂O, 1500 mg/kg; lead: Pb(NO₃)₂, 5000 mg/kg				
Duration (h)	100				
Anodic and cathodic electrolyte solutions	KNO₃ (0.01 M)				

Fig. 6. Variation of pH in the soil bed after experiments: (a) rectangular reactor: test 1 (control) and test 2 (IEM-enhanced); (b) cylindrical reactor: test 3 (control), test 4 (IEM-enhanced, without ASC), and test 5 (IEM-enhanced, with ASC).

Fig. 7. Variation of pH in the auxiliary solution cell (ASC); test 5 (cylindrical, IEM-enhanced, and with ASC).

decrease of the effectiveness of the remediation technology: (1) metal precipitation; (2) increase of adsorbed and immobile metal species; (3) clogging of soil pores by precipitates that result in a decrease in electroosmotic flow. As a consequence, a number of enhancement schemes have been proposed to overcome these obstacles [7,9,24]. IEM-enhanced tests were conducted in this study in order to acquire a basic concept of enhancement schemes and to understand the principal mechanisms involved in enhancement processes. The soil pH values of the cathodic region in the control tests (tests 1 and 3) were near 12, whereas those in the IEM-enhanced tests (tests 2, 4 and 5) were below 7 (Fig. 6), even though the pHs in the catholyte solutions of each test were in the range of 12 and 13 (the data not shown). Furthermore, the overall soil pHs in IEM-enhanced tests were lower than those in the control tests, except for pHs recorded close to the anode which experienced direct leakage of the acidic anolyte through the filter during the control test. The AEM placed in the anodic part prevented cations such as K^+ from entering into the soil cell, and no current was wasted for carrying cations from anode to cathode. However, the hydrogen ions generated in the anodic electrolysis of water can pass the AEMs. Because of the molecular interaction of water dipoles with electrical charges, protons form hydronium-ions with the water. In a
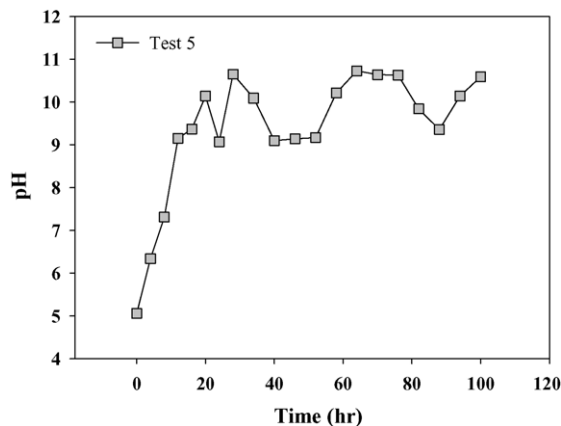
hydronium ion, the three attached H-atoms are no longer distinguishable in terms of their electric charges. They form a tripod with three H-atoms equally apart carrying the positive charge together. The formation of the hydronium ions has consequences for the mobility of the protons in aqueous media. Common salt ions move with their hydrate shell through the solution. The proton, however, is transported mostly via a so-called tunnel mechanism from one hydronium-ion to the next water molecule. This explains not only the extraordinary high mobility of protons but also the high permeability of AEMs for protons while these membranes generally have a very low permeability for salt cations. Therefore, the pH of the soil bed in anodic part decreased even in the IEM-enhanced tests (tests 2, 4, and 5 in Fig. 6).

The auxiliary solution cell (ASC) was placed between the soil bed and cathodic compartment in test 5. The pH variation of the ASC is shown in Fig. 7. ASC pHs were lower (about 9–11) than those of cathodic electrolytes (about 12–13, detailed data not presented). Even though the hydroxide ions migrated into the ASC through the holes in the CEMs, the amount of these ions in the ASC was smaller than that recorded for the cathodic electrolytes. In addition, the hydroxide ions were consumed continuously through metal precipitation occurring in the ASC. It is for these reasons that the pH in the ASC was slightly lower than that in the cathodic electrolytes.

The voltage drops within the CEMs in the IEM-enhanced tests are shown in Fig. 8. Among three IEM-enhanced experiments (tests 2, 4 and 5), the ASC was placed only in test 5. In tests 2 and 4 without the ASC, voltage drops within the CEMs suddenly increased after approximately 40 h of processing time and implies that metal hydroxide precipitation was initiated within the CEMs and subsequently clogged the CEM pores. However, the sudden increase of voltage drops was not observed in test 5 with the ASC. The voltage profiles within the CEMs in the IEM-enhanced tests indicate that fouling phenomena can be prevented by using the ASC.

The distribution of residual metal concentrations in the soil bed after experiments is shown in Figs. 9 and 10. The
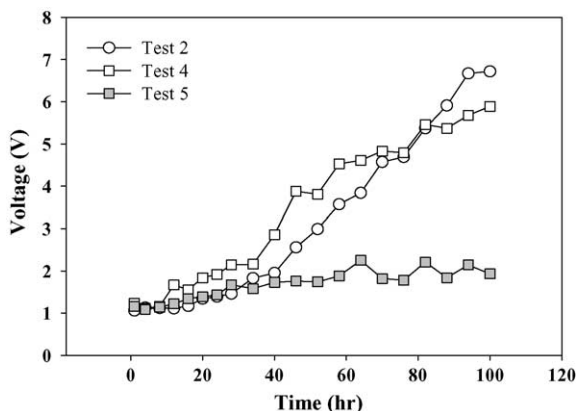
Fig. 8. Voltage profiles within the CEMs of the IEM-enhanced tests: test 2 (rectangular, IEM-enhanced), test 4 (cylindrical, IEM-enhanced, without ASC), and test 5 (cylindrical, IEM-enhanced, with ASC).

residual metal concentrations were increasing significantly towards the cathode in all tests. In particular, the residual concentration in the control tests (tests 1 and 3) appeared as high as 3–4 times the initial metal concentrations of the soil fraction near the cathode. In the rectangular configura-
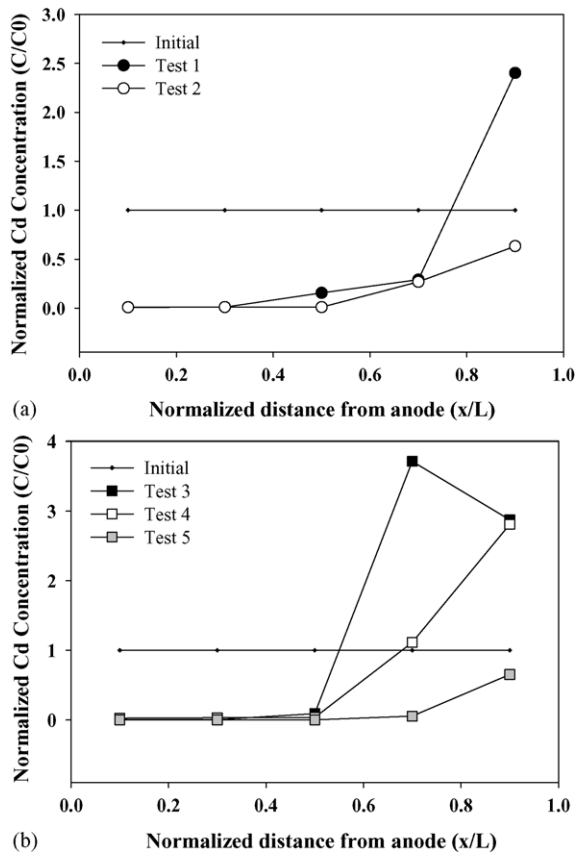

Fig. 9 Distribution of residual. Cd concentrations within the soil bed after experiments: (a) rectangular reactor: test 1 (control) and test 2 (IEM-enhanced); (b) cylindrical reactor, test 3 (control), test 4 (IEM-enhanced, without ASC), and test 5 (IEM-enhanced, with ASC) (C_0 = initial Cd concentration, C = final Cd concentration, x = distance from anode, L = length of soil bed).
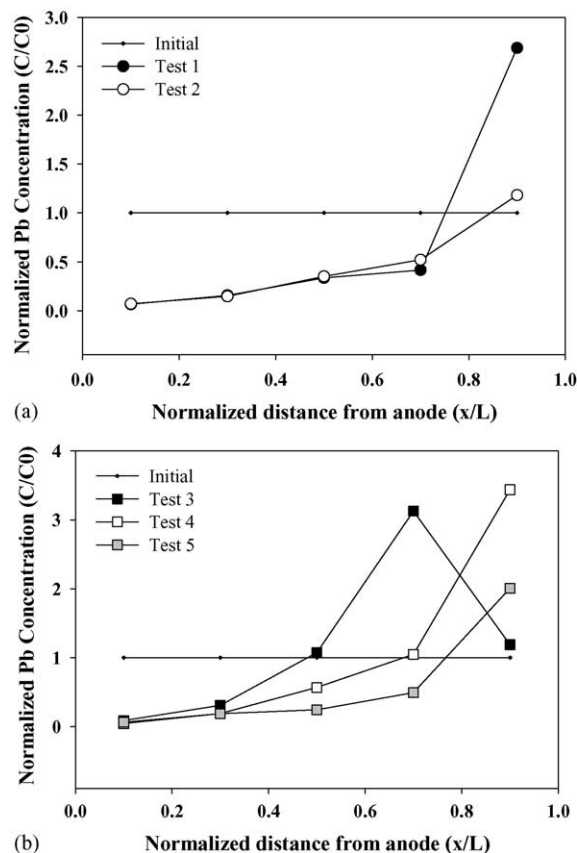

Fig. 10. Distribution of residual Pb concentrations within the soil bed after experiments: (a) rectangular reactor; test 1 (control) and test 2 (IEM-enhanced), (b) cylindrical reactor; test 3 (control), test 4 (IEM-enhanced, without ASC), and test 5 (IEM-enhanced, with ASC) (C_0 = initial Pb concentration, C = final Pb concentration, x = distance from anode, L = length of soil bed).

tion experiments (tests 1 and 2), it is clear that the residual concentrations of metal contaminants in the region near the cathode were much lower in the IEM-enhanced test (test 2) than in the control test (test 1). This indicates that hydroxide precipitation was prevented by the lack of introduction of hydroxyl ions from the cathode compartment into the soil bed, resulting from the insertion of cation exchange membranes (CEMs) between the soil bed and cathode electrolyte.

A comparison of the profiles of residual metal concentrations between tests 4 and 5 in Figs. 9 and 10 elucidates the role played by the ASC. As mentioned previously, the fouling phenomena within the CEM was inferred from the voltage profile of the CEM (Fig. 8). In order to prevent fouling phenomena within the CEM in the cylindrical reactor, the ASC was placed between the soil bed and cathode compartment (see test 5 in Table 3). As shown in Fig. 7, pHs of the ASC increased to 9–11 as a result of migration of hydroxide ions from the cathode electrolyte solution into the ASC through the holes designed on the CEM surface. Accordingly, hydroxide metal precipitation occurred within the ASC and not in the CEM, and the fouling phenomena could be prevented. As a result, a comparison of the removal efficiencies between

Table 4
The removal efficiency of each test (%)

	Rectangular configuration		Cylindrical configuration		
	Test 1	Test 2	Test 3	Test 4	Test 5
Cd	42.64	81.42	22.30	59.15	91.60
Pb	26.74	54.46	14.19	39.75	58.44

tests 4 and 5 as shown in Table 4 reveals that the removal of metal contaminants was significantly improved. In addition, the residual metal concentrations were much lower at the region near the cathode in the test with an ASC (test 5) than in the test without an ASC (test 4) under equivalent operational conditions, as shown in Figs. 9 and 10.

The residual concentrations of heavy metals in the region near the cathode differed when comparing rectangular and cylindrical configurations. In the case of control tests (tests 1 and 3), the peaks of the residual metal concentrations of the cylindrical configurations appeared at a region relatively distant from the cathode (normalized distance from the anode: 0.7) in comparison to those of the rectangular configurations (normalized distance from the anode: 0.9), as shown in Figs. 9 and 10. In particular, significant increases in residual metal concentrations were observed at a region near the cathode in cylindrical IEM-enhanced tests. These increases in concentration did not occur in the rectangular configuration experiment, as shown by a comparison of the concentration profiles between tests 2 and 4 in Figs. 9 and 10. All the differences in the residual metal concentration distributions between rectangular and cylindrical configurations may be caused by the change in the cross-sectional area in the cylindrical configuration. The change in the cross-sectional area results in a change in the current density and metal flux at local points in the soil bed. Since a constant current was applied over the duration of both rectangular and cylindrical configuration experiments, the current density was kept constant in

the whole rectangular reactor but changed at each location in the cylindrical reactor, becoming lower and higher at regions near the anode and cathode, respectively. Accordingly, the overall removal efficiencies of the cylindrical configuration were lower than those of the rectangular configuration (see Table 4), as evidenced by the fact that the residual metal concentrations were generally higher in the cylindrical configuration than in the rectangular configuration since the initiation of metal transport may have been delayed due to a lower current density at the region near the anode. Furthermore, the gradual increase in the metal flux towards the cathode in the cylindrical configuration results in residual metal concentration distributions that differ from those in the rectangular configuration, particularly at the region near the cathode. As a result of the decrease in cross-sectional area and subsequent increase in the metal flux in the cylindrical reactor, the metal contaminants were concentrated and accumulated at a region near the cathode, and residual metal concentrations appeared significantly higher than those in the rectangular reactor, even though hydroxide precipitation was prevented by cation exchange membranes in the cylindrical IEM-enhanced experiments. However, the concentrated metal contaminants at the region near the cathode ought to be removed easily by IEM-enhanced processing if the duration of the experiment is extended in cylindrical configuration tests. This prediction is based on an analysis of the differences in concentration profiles between a control test (test 1) and IEM-enhanced test (test 2) in rectangular configuration experiments (Figs. 9 and 10), from which it is clear that the concentration and accumulation of metal contaminants is not caused by the hydroxide precipitation.

The removal efficiencies of Cd and Pb were significantly different, with the removal efficiencies of Pb being much lower than those of Cd in all tests (Table 4). This may be a result of the different geochemical characteristics of Cd and Pb. Lead has a much higher affinity for kaolinite surfaces

Table 5
The mass balances of each test

	Metal species	Amount of metal (mg)					Recovery (%)[c]
		Initial (a)	Remained in the soil bed (b)	Accumulated in electrolytes (c)	Existed in the other parts (d)[a]	Total measured (e)[b]	
Test 1	Cd	2876.0	1649.1	819.20	163.10	2631.4	91.50
	Pb	9736.0	7132.6	1607.2	275.40	9015.2	92.60
Test 2	Cd	2876.0	534.40	1769.5	176.70	2480.6	86.25
	Pb	9736.0	4433.8	4116.2	301.90	8851.9	90.92
Test 3	Cd	8643.0	6715.6	902.10	293.20	7910.9	91.53
	Pb	29517	25329	2714.6	374.30	28417	96.27
Test 4	Cd	8643.0	3530.7	3751.1	292.10	7573.9	87.63
	Pb	29517	17784	8394.1	389.80	26568	90.01
Test 5	Cd	8643.0	726.00	6645.7	251.40	7623.1	88.20
	Pb	29517	12267	15537	361.50	28166	95.42

[a] The amount of metals existed in the other parts includes those in reactor walls, tubes, and electrodes.
[b] Total measured = (a) + (b) + (c).
[c] Recovery (%) = [(e)/(a)] × 100.

than Cd, and Pb is retained significantly by kaolinite even in conditions of low pH [3,9,10]. This may explain why the migration of Pb was delayed and the removal efficiency of Pb decreased.

The mass balance was checked in each test and the results are summarized in Table 5. After each test, recoveries of metal species were in the range of 86–96%. In addition, power consumptions of each test were calculated. In the rectangular configuration, 417 and 334 kWh/t were consumed during tests 1 and 2, respectively. The power consumptions in the cylindrical configuration were 1246 kWh/t for test 3, 1019 kWh/t for test 4, and 671 kWh/t for test 5.

4. Conclusions

One of the major drawbacks of using conventional (unenhanced) electrokinetic (EK) soil processing to remove heavy metal contaminants involves hydroxide precipitation in the soil fraction near the cathodic electrode. In an effort to overcome this defect, electrodialytic soil processing in the form of EK soil processing enhanced with ion exchange membranes (IEMs) was evaluated for its efficiency in removing Cd and Pb from artificially contaminated kaolinite. Additionally, the auxiliary solution cell (ASC) was tested to prevent fouling phenomena occurring within the cation exchange membranes (CEMs) used in the IEM-enhanced EK processing. Furthermore, the efficacy of electrode configurations was investigated using two different configurations of electrode: rectangular and cylindrical. The overall removal efficiencies of the IEM-enhanced EK tests were much higher than those of conventional (unenhanced) EK tests due to the prevention of hydroxide precipitation in the soil bed and increase in current efficiency. However, fouling phenomena within the CEM were readily observed during IEM-enhanced EK processing. In order to prevent fouling phenomena within the CEM, an ASC was inserted between the soil bed and cathode compartment, and the removal efficiencies increased owing to the use of the ASC. Apparent removal efficiencies of the cylindrical reactor were lower than those of the rectangular reactor in IEM-enhanced EK processing due to the change in cross-sectional area of the cylindrical reactor, but the removal efficiency of the cylindrical reactor could increase if the duration of processing is extended since it was clear that the concentration and accumulation of metal contaminants was not caused by hydroxide precipitation. The cylindrical configuration of the processing technique can therefore be implemented in practical situations to improve the treatability of cathode effluent containing a high level of contaminants after processing.

Acknowledgements

References

[1] A.M.O. Mohamed, Development of a novel electro-dialysis based technique for lead removal from silty clay polluted soil, J. Hazard. Mater. 90 (2002) 297–310.

[2] D.C. Adriano, Trace Elements in Terrestrial Environments, Springer-Verlag, New York, 1986, pp. 7–14.

[3] S.O. Kim, S.H. Moon, K.W. Kim, Removal of heavy metals from soils using enhanced electrokinetic soil processing, Water Air Soil Pollut. 125 (2001) 259–272.

[4] S. Pamukcu, J.K. Wittle, Electrokinetically enhanced in situ soil decontamination, in: D.L. Wise, D.J. Trantolo (Eds.), Remediation of Hazardous Waste Contaminated Soils, Marcel Dekker, New York, 1994, pp. 245–298.

[5] R. Lageman, Electro-reclamation: applications in the Netherlands, Environ. Sci. Technol. 27 (1993) 2648–2650.

[6] Y.B. Acar, R.J. Gale, A.N. Alshawavkeh, Electrokinetic remediation: basics and technology status, J. Hazard. Mater. 40 (1995) 117–137.

[7] C.N. Hsu, Electrokinetic remediation of heavy metal contaminated soils, Ph.D. Thesis, Texas A&M University, College Station, TX, 1997.

[8] A.N. Alshawabkeh, A.T. Yeung, M.R. Bricka, Practical aspects of in-situ electrokinetic extraction, J. Environ. Eng. 125 (1999) 27–35.

[9] S.O. Kim, Electrokinetic remediation of heavy metal contaminated soils and sludges, Ph.D. Thesis, Gwangju Institute of Science and Technology, Gwangju, Republic of Korea, 2001.

[10] S.O. Kim, K.W. Kim, D. Stüben, Evaluation of electrokinetic removal of heavy metals from tailing soils, J. Environ. Eng. 128 (2002) 705–715.

[11] S.O. Kim, S.H. Moon, S.T. Yun, K.W. Kim, Pilot scale study on the ex situ electrokinetic removal of heavy metals from municipal wastewater sludges, Water Res. 36 (2002) 4765–4774.

[12] Y.B. Acar, A.N. Alshawabkeh, Principles of electrokinetic remediation, Environ. Sci. Technol. 27 (1993) 2638–2647.

[13] R.F. Probstein, R.E. Hicks, Removal of contaminants from soils by electric fields, Science 260 (1993) 498–503.

[14] T. Rødsand, Y.B. Acar, G. Breedveld, Electrokinetic Extraction of Lead from Spiked Norwegian Marine Clay: Characterization, Containment, Remediation, and Performance in Environmental Geotechnics, Geotechnical Special Publication, ASCE, New York, 1995.

[15] S. Pamukcu, L.I. Khan, H.-Y. Fang, Zinc detoxification of soils by electroosmosis, in: Geotechnical Engineering Transportation Research Record 1288, Transportation Research Board, National Research Council, Washington, DC, USA, 1990, pp. 41–46.

[16] A.P. Shapiro, R. Probstein, Removal of contaminants from saturated clay by electroosmosis, Environ. Sci. Technol. 27 (1993) 283–291.

[17] G.R. Eykholt, D.E. Daniel, Impact of system chemistry on electroosmosis in contaminated soils, J. Geotech. Eng. ASCE 120 (1994) 797–815.

[18] G.R. Eykholt, Driving and complicating features of electrokinetic treatment of soils, Ph.D. Thesis, University of Texas at Austin, Austin, TX, 1992.

[19] L.J. West, D.I. Stewart, Effect of Zeta Potential on Soil Electrokinesis: Characterization, Containment, Remediation, and Performance in Environmental Geotechnics, Geotechnical Special Publication, ASCE, New York, 1995, pp. 1535–1549.

[20] A.T. Yeung, C. Hsu, R.M. Menon, EDTA-enhanced electrokinetic extraction of lead, J. Geotech. Eng. ASCE 122 (1996) 666–673.

[21] E.G. Lee, S.H. Moon, Y.K. Chang, I.K. Yoo, H.N. Chang, Lactic acid recovery using two-stage electrodialysis and its modeling, J. Membr. Sci. 145 (1998) 53–66.

[22] H.J. Lee, J.M. Choi, J.W. Cho, S.H. Moon, Characterization of anion exchange membranes fouled with humate during electrodialysis, J. Membr. Sci. 203 (2002) 115–126.

[23] J.K. Mitchell, Fundamentals of Soil Behavior, Wiley, New York, 1993.

[24] A.N. Alshawabkeh, Theoretical and experimental modeling of removing contaminants from soils by an electric field, Ph.D. Thesis, The Louisiana State University, Baton Rouge, LA, 1994.